Structural Basis for Recognition of the Intron Branch Site RNA by Splicing Factor 1

Zhihong Liu,[1]* Ingrid Luyten,[1]* Matthew J. Bottomley,[1] Ana C. Messias,[1] Sophie Houngninou-Molango,[2] Remco Sprangers,[1] Katia Zanier,[1] Angela Krämer,[2] Michael Sattler[1]†

During spliceosome assembly, splicing factor 1 (SF1) specifically recognizes the intron branch point sequence (BPS) UACUAAC in the pre-mRNA transcripts. We show that the KH-QUA2 region of SF1 defines an enlarged KH (hn RNP K) fold which is necessary and sufficient for BPS binding. The 3′ part of the BPS (UAAC), including the conserved branch point adenosine (underlined), is specifically recognized in a hydrophobic cleft formed by the Gly-Pro-Arg-Gly motif and the variable loop of the KH domain. The QUA2 region recognizes the 5′ nucleotides of the BPS (ACU). The branch point adenosine acting as the nucleophile in the first biochemical step of splicing is deeply buried. BPS RNA recognition suggests how SF1 may facilitate subsequent formation of the prespliceosomal complex A.

The removal of introns from pre-mRNA transcripts is catalyzed by the spliceosome (*1*). Initial spliceosome assembly in higher eukaryotes involves cooperative binding of SF1 [or branch point binding protein (BBP)] and U2 auxiliary factor (U2AF) to intron sequences upstream of the 3′ splice site (*2, 3*). SF1 specifically recognizes the BPS which is almost invariant in *Saccharomyces cerevisiae* (UACUAAC), but more divergent in mammals (YNCURAY; Y, pyrimidine; R, purine; N, any nucleotide; the branch point adenosine is underlined) (*4*). SF1 belongs to the STAR (signal transduction and activation of RNA) (*5*) family of proteins, which share a conserved region, QUA2 (Quaking homology 2) located COOH-terminal to a KH domain (*6*). We found that the KH-QUA2 region of SF1 adopts an enlarged KH fold which is necessary and sufficient for BPS binding. The BPS recognition involves numerous STAR-specific amino acids and is consistent with mutations that affect RNA binding in vitro and splicing (*4, 7*). The SF1/BPS structure suggests how SF1 may facilitate spliceosome assembly.

The KH-QUA2 region and a zinc knuckle (Zn) located further COOH-terminal have been implicated in branch site RNA binding (*3, 7, 8*). Here, we have defined the minimal region of human SF1 required for RNA recognition by nuclear magnetic resonance (NMR) titration experiments with 5′-UAUACUAACAA (BPS RNA). This RNA contains the *S. cerevisiae* BPS (underlined), which also represents the preferred BPS in mammals (*9*). Addition of BPS RNA to proteins encompassing the KH-QUA2 region of SF1 induces extensive changes in the NMR spectra as expected for the formation of a stable protein/RNA complex (Fig. 1). Additional experiments demonstrate that the KH-QUA2 region of SF1 is necessary and sufficient for recognition of the BPS RNA (*6*). Based on isothermal titration calorimetry, the dissociation constant for the KH-QUA2/BPS RNA complex is ≈1 μM, consistent with previous reports (*3*).

The three-dimensional (3D) structure of the KH-QUA2/BPS RNA complex was determined using heteronuclear multidimensional NMR spectroscopy (*10*). Recombinant ^{13}C,^{15}N-labeled SF1 KH-QUA2 was complexed with unlabeled BPS RNA. Distance restraints were derived from 3D ^{15}N- and ^{13}C-edited NOE spectra. RNA assignments and intermolecular protein/RNA distance restraints were obtained from filtered 2D and 3D experiments (*11, 12*). The structure is very well defined by the NMR data, which include about 300 intermolecular distance restraints involving 28 amino acids and 9 nucleotides. An ensemble of 15 NMR structures and a ribbon representation of the lowest energy structure are shown in Fig. 2A.

The structure of the SF1 KH domain resembles that of other KH domains [rmsd ≈ 2.8 Å with Nova2 KH3 (*13*) and Vigilin (*14*)] consistent with the conservation of hydrophobic residues (*6*) stabilizing the KH domain fold (Fig. 2B). Residues 239 to 249 of QUA2 define an amphipathic helix (α4) that forms a hydrophobic interface with helices α1 (L155), α3 (I225) and the GPRG loop (P159) of the KH domain (Fig. 2B). Based on secondary chemical shifts (*15*), the secondary structure of KH-QUA2, including α4, is preformed and not induced by RNA binding. The sequence conservation of hydrophobic core residues in the KH and QUA2 regions (*6*) suggests a similar β1-α1-α2-β2-β3-α3-α4 topology for all STAR family proteins. Thus, the KH-QUA2 region of STAR proteins defines a novel enlarged KH fold.

The 5′ and 3′ ends of the RNA interact with the COOH- and NH_2-terminal regions of the KH-QUA2 protein, respectively (Fig. 2). The BPS RNA adopts an extended single-stranded conformation and is bound in a hydrophobic groove between QUA2, the GPRG loop, and the variable loop of the KH domain. Helices α1 and α2 and strand β2 of the KH domain, and conserved residues in the QUA2 region interact with the RNA (Figs. 2 and 3). The large RNA binding surface (solvent-accessible surface area buried upon complex formation ≈2500 Å^2) is very hydrophobic (Fig. 2C), due to numerous conserved aliphatic side chains that are located at the surface of the protein. In addition, conserved positively charged side chains flanking the hydrophobic RNA binding groove form

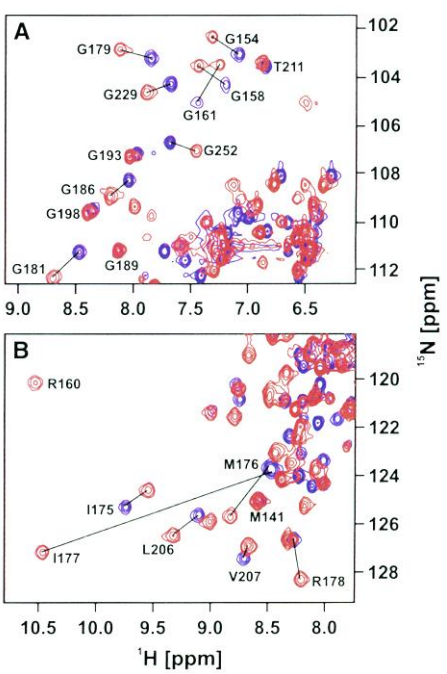

Fig. 1. The KH-QUA2 region of SF1 binds to the BPS RNA. In (**A**) and (**B**), two well-resolved regions of ^{1}H,^{15}N correlation spectra for SF1 KH-QUA2 are shown in the absence (blue) and presence (red) of BPS RNA. Amino acid assignments are indicated. The backbone amide signals of R160 in the Gly-Pro-Arg-Gly motif and of I177 in strand β2 (B) experience very large chemical shift changes upon RNA binding consistent with their involvement in hydrogen bonding to Ura6 and the branch point adenosine Ade8 in the BPS RNA, respectively (Fig. 3).

[1]European Molecular Biology Laboratory (EMBL), Meyerhofstraße 1, D-69117 Heidelberg, Germany. [2]University of Geneva, Department of Cell Biology, CH-1211 Geneva 4, Switzerland.

*These authors contributed equally to this work.
†To whom correspondence should be addressed. E-mail: sattler@EMBL-Heidelberg.de

compensating electrostatic interactions with the solvent-exposed phosphate backbone of the RNA (Figs. 2C and 3).

The KH-QUA2/BPS RNA complex is stabilized by a combination of hydrophobic interactions, hydrogen bonding, and electrostatic contacts (Fig. 3A). Consistent with the conservation of the branch point adenosine in the BPS, Ade8 is specifically recognized by the KH

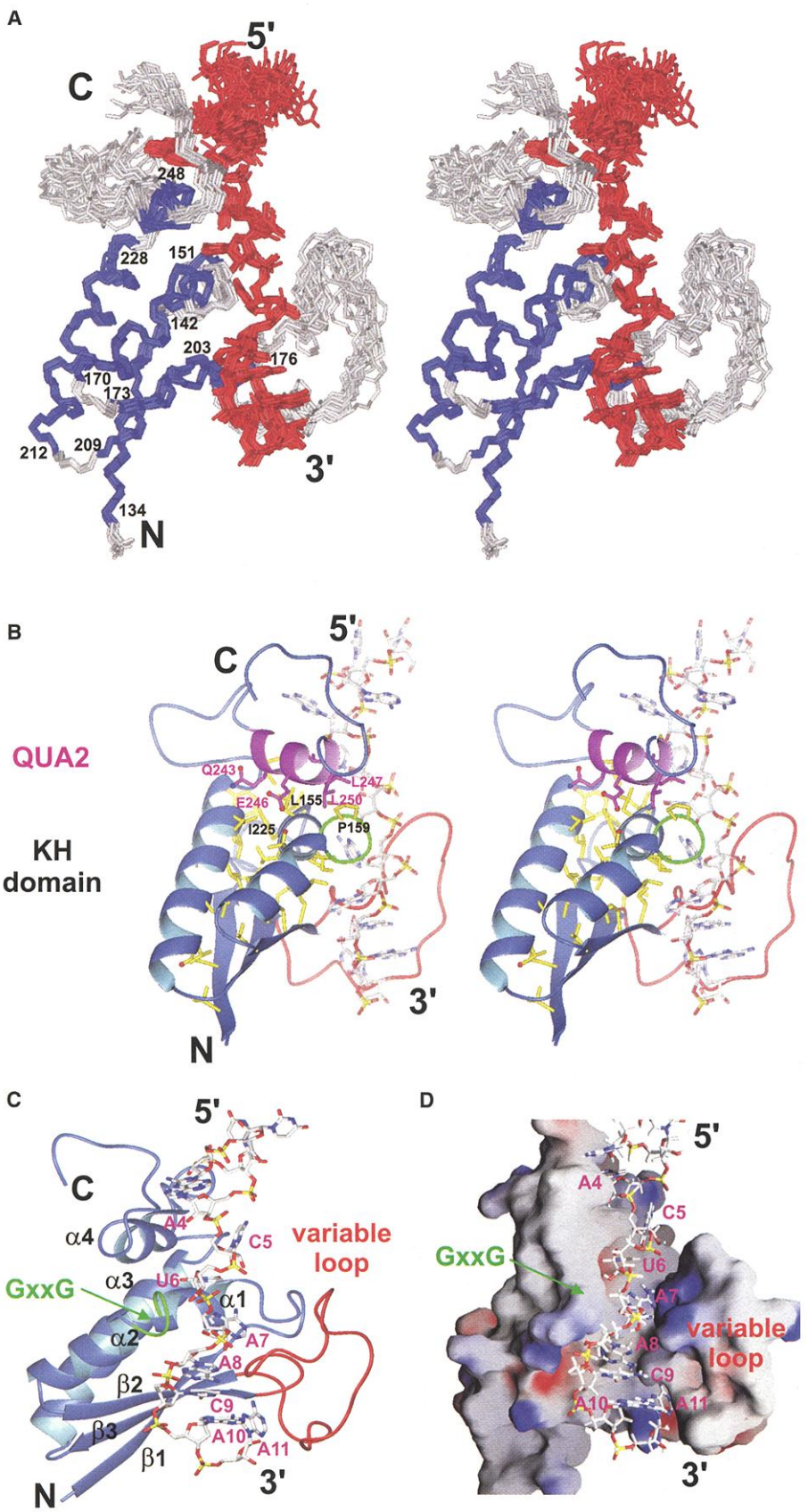

Fig. 2. Structure of the SF1/branch site RNA complex. **(A)** Stereoview of the NMR ensemble of the SF1 KH-QUA2/BPS RNA complex. RNA heavy atoms are shown in red; the N, Cα, C′ trace of the protein is shown in gray and colored blue for secondary structure elements. **(B)** Ribbon representation of the SF1 KH-QUA2 domain bound to the BPS. Side chains of conserved hydrophobic core residues are shown in yellow; residues in the KH/QUA2 interface and the QUA2 helix α4 are colored magenta. The Gly-Pro-Arg-Gly motif and the variable loop of the KH domain are colored green and red, respectively. **(C)** Ribbon and **(D)** surface representation of the KH-QUA2/BPS complex. Secondary structure elements of the KH-QUA2 protein are labeled; RNA nucleotides are colored by atom type and annotated in magenta. The surface of the KH-QUA2 region is colored white, blue, and red for neutral, positive, and negative electrostatic potential, respectively.

domain. Most remarkably, the N6 and N1 of Ade8 form hydrogen bonds with the backbone amide and carbonyl oxygen of I177, which mimic the Watson-Crick functional groups of a uridine. Another hydrogen bond is found between the 2′ hydroxyl of Ade7 and the N7 of Ade8. In combination, this pattern of hydrogen bonds uniquely specifies an adenosine base at this position. Consistently, the branch point adenosine is strictly conserved, and mutation to any other base abolishes SF1 binding (*4*). The sugar puckers and base stacking between Ade8, Cyt9, and Ade10 resemble an A-helical conformation. Ade8 is surrounded by conserved aliphatic side chains (I157, L164, I175, I177, V183) of the KH domain (Fig. 3B). A L164N mutation in SF1 decreases the RNA binding affinity by 50% (*7*). The L164N mutation directly destabilizes the RNA interaction and does not affect the 3D fold of the KH domain [based on NMR spectra (*15*)]. In contrast, the corresponding mutation in KH2 of FMR1, which is associated with the Fragile X syndrome, affects the KH fold in vitro (*16, 17*).

A potential π-cation interaction (*18*) between the Ade7 base and the side chain of K184 (Fig. 3C) is consistent with the preference for purine bases at this position in both the *S. cerevisiae* and mammalian branch sites. A K184A mutation abolishes RNA binding (Fig. 4), demonstrating the importance of this interaction. The phosphates of Ade7 and Ade8 closely approach the peptide backbone near the ^{158}GPRG^{161} loop. Consequently, a G161D mutation almost eliminates RNA binding (*7*), and mutation (R160E) of the R160 side chain, which contacts the 3′ phosphate of the branch point adenosine (Ade8) (Fig. 3B), severely reduces RNA binding (Fig. 4). The N6 of Ade7 interacts with the side chain of the conserved E149, which is positioned via a hydrogen bond with the backbone amide of I150 (Fig. 3C).

Analysis of the structure also explains the conservation of Ura6 in the BPS. Ura6 is located at the interface between the KH and QUA2 domains (Fig. 3D). The Ura6 base interacts with L244 and L247 in the QUA2 helix (α4) and closely approaches the peptide backbone of helix α1 consistent with the conservation of G154. The imino proton of Ura6 is positioned to form a hydrogen bond with the backbone amide of L155. Together with steric constraints, these interactions are specific for uridine, consistent with the conservation of this nucleotide and the loss of SF1 binding with a Ura6Ade mutant branch site (*4*). The sugar of Ura6 stacks with P159 in the GPRG loop and is stabilized by a hydrogen bond between its 2′-OH and the backbone amide of R160 (Fig. 3D). Both the sugar and base of Cyt5 exhibit numerous hydrophobic contacts with the exposed aliphatic side chains of L244 and L247. Consistent with this, the L244A or L247A mutations decrease the RNA interaction (Fig. 4). N151 is positioned to recognize the Watson-Crick face of Cyt5, consistent with reduced RNA binding of a N151A mutant protein (Fig. 4). Residues in the QUA2 region (L244, L247, T253, L254, R255) interact with Ade2, Ade4, and Cyt5. These interactions seem less important, because mutation of Ade4 or Cyt5 to guanosine in the BPS (*4*), or the L254A and R255A mutations in KH-QUA2 (Fig. 4), have smaller effects on SF1 binding.

The structure described herein provides the first example for sequence-specific recognition of the conserved single-stranded BPS RNA. The complex of the Nova2-KH3 domain bound to a stem-loop RNA (*13*) is the only other high-resolution structure showing RNA recognition by a KH domain in the absence of a QUA2 domain. In both complexes the protein/RNA interfaces are very hydrophobic, but aromatic residues are not used for RNA recognition. These are likely to be general features of KH domain/RNA interactions considering the conservation of aliphatic amino acids and the low abundance of aromatic residues in KH domains. In contrast, the recognition of single-stranded RNA by RNP domains always employs conserved aromatic residues for stacking interactions with RNA bases (*19, 20*). Interestingly, the recognition of Ura6-Ade7-Ade8-Cyt9 by SF1 resembles the interaction of Ura12-Cyt13-Ade14-Cyt15 by the Nova2-KH3 domain (*13*). Notably, the Watson-Crick recog-

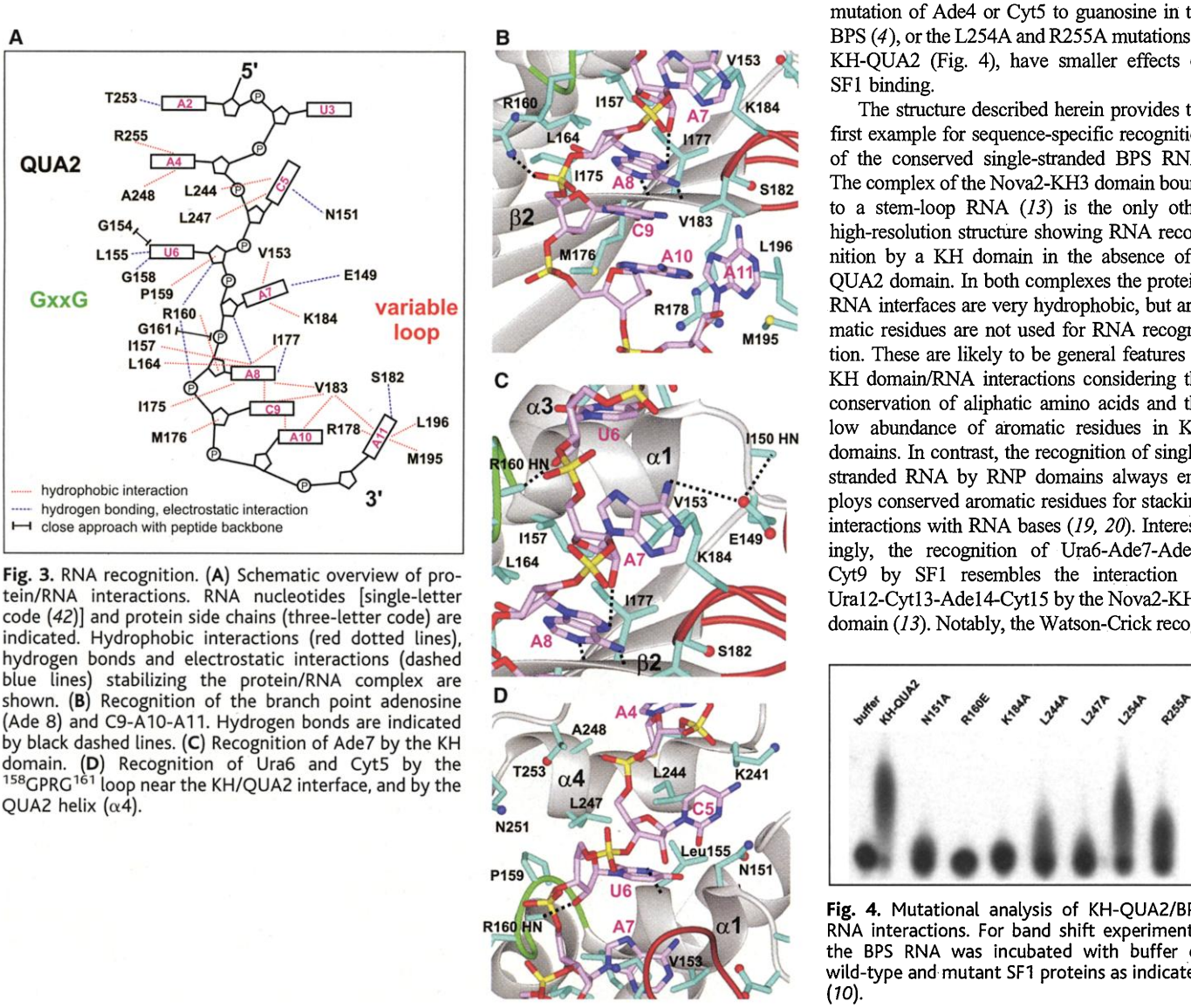

Fig. 3. RNA recognition. (**A**) Schematic overview of protein/RNA interactions. RNA nucleotides [single-letter code (*42*)] and protein side chains (three-letter code) are indicated. Hydrophobic interactions (red dotted lines), hydrogen bonds and electrostatic interactions (dashed blue lines) stabilizing the protein/RNA complex are shown. (**B**) Recognition of the branch point adenosine (Ade 8) and C9-A10-A11. Hydrogen bonds are indicated by black dashed lines. (**C**) Recognition of Ade7 by the KH domain. (**D**) Recognition of Ura6 and Cyt5 by the ^{158}GPRG^{161} loop near the KH/QUA2 interface, and by the QUA2 helix (α4).

Fig. 4. Mutational analysis of KH-QUA2/BPS RNA interactions. For band shift experiments, the BPS RNA was incubated with buffer or wild-type and mutant SF1 proteins as indicated (*10*).

nition of adenosine by two hydrogen bonds with the peptide backbone is mediated by equivalent positions in the β2 strand of the KH domains (*21*). However, BPS RNA binding by SF1 requires the QUA2 region in addition to the KH domain. Thus, the enlarged KH fold defined by the KH-QUA2 region is crucial for sequence-specific recognition of the single-stranded 7-nucleotide BPS RNA (*22*).

The structure of the SF1/RNA complex provides insight into early steps of spliceosome assembly. (i) It has been shown that binding of U2AF65 to the polypyrimidine tract, located downstream of the BPS, directs its Arg-Ser–rich (RS) domain to contact the branch site (*23*). The structure presented herein is compatible with this and suggests that the positively charged RS domain could interact with the solvent-exposed, negatively charged phosphate backbone of the BPS. (ii) Our NMR titrations show that the SF1 zinc knuckle does not contact the BPS. Thus, in contrast to a previously suggested model (*8*), we expect that the zinc knuckle may interact with nucleotides located upstream of the BPS in the pre-mRNA. (iii) The most striking feature of the SF1/BPS RNA complex structure is that the branch point adenosine (Ade8) is deeply buried in a hydrophobic pocket of the KH domain. The base of Ade8 is oriented towards the protein and stabilized by two hydrogen bonds with the peptide backbone, and thus shielded from interaction with other molecules. The next step of spliceosome assembly involves the formation of a BPS/U2 snRNA duplex (complex A), in which the branch point adenosine is bulged out (*24, 25*). For duplex formation, the complementary U2 snRNA presumably approaches the SF1/BPS complex from its accessible, open face (Fig. 2C). The burial of the Ade8 base constrains it in an orientation that favors its exclusion from the duplex with the U2 snRNA. Even though formation of the BPS/U2 snRNA duplex requires disruption of the SF1/BPS complex, the recognition of Ade8 in a "prebulged" conformation is likely to facilitate this transition and could explain the kinetic effects of SF1 during spliceosome assembly (*26, 27*). (iv) Protein/RNA recognition in the SF1/BPS complex may provide a structural basis for human inherited diseases that result from intronic mutations of Ura6 or Ade8 in the BPS (*28, 29*).

References and Notes

1. A. Krämer, *Annu. Rev. Biochem.* **65**, 367 (1996).
2. N. Abovich, M. Rosbash, *Cell* **89**, 403 (1997).
3. J. A. Berglund, N. Abovich, M. Rosbash, *Genes Dev.* **12**, 858 (1998).
4. J. A. Berglund, K. Chua, N. Abovich, R. Reed, M. Rosbash, *Cell* **89**, 781 (1997).
5. C. Vernet, K. Artzt, *Trends Genet.* **13**, 479 (1997).
6. Supplementary materials showing a multiple sequence alignment of STAR family proteins and NMR titration experiments are available at *Science* Online at www.sciencemag.org/cgi/content/full/294/5544/1098/DC1.
7. J. C. Rain, Z. Rafi, Z. Rhani, P. Legrain, A. Krämer, *RNA* **4**, 551 (1998).
8. J. A. Berglund, M. L. Fleming, M. Rosbash, *RNA* **4**, 998 (1998).
9. Y. A. Zhuang, A. M. Goldstein, A. M. Weiner, *Proc. Natl. Acad. Sci. U.S.A.* **86**, 2752 (1989).
10. The KH-QUA2 region (residues 134 to 260) of human SF1 was cloned into a modified pET24d expression vector (Novagen) containing an NH_2-terminal histidine-tag followed by a TEV protease cleavage site. SF1 mutants were prepared using the QuickChange site-directed mutagenesis kit (Stratagene). Uniformly ^{15}N-labeled and ^{15}N- and ^{13}C-labeled proteins were prepared by growing the *Escherichia coli* strain BL21(DE3) overexpressing KH-QUA2 in a minimal medium containing $^{15}NH_4Cl$ with or without uniformly ^{13}C-labeled glucose. Recombinant proteins were purified on a Ni-chelating affinity column. The histidine-tag was removed by TEV protease cleavage and additional purification was achieved with chromatography on a Q-Sepharose column. The BPS RNA 5′-UAUACUAACAA was synthesized in-house or purchased from Biospring, Frankfurt, Germany. Samples for NMR contained a 1:1 complex of KH-QUA2 and the RNA at a concentration of 1 mM in 20 mM sodium phosphate buffer (pH 6.5), 50 mM NaCl, 2 mM dithiothreitol. For NMR titrations, ^{15}N-labeled samples comprising the KH (residues 134 to 229) and KH-QUA2-Zn regions (residues 134 to 296) of human SF1 were prepared as described above. To determine RNA binding, band-shift experiments were performed in 10-μl reactions containing 20 mM tris-HCl (pH 8.0), 100 mM NaCl, 5 mM imidazole, 2.5 mM β-mercaptoethanol, 2.5 μg tRNA, 2 μg of KH-QUA2 or mutant proteins, and 0.01 pmol 5′ [^{32}P]ATP-labeled BPS RNA. After 15 min at room temperature, reaction products were separated in a 6% polyacrylamide gel (acrylamide:bisacrylamide, 80:1) in 25 mM tris, 25 mM boric acid, and 1 mM EDTA at 4°C. Reaction products were visualized by autoradiography. NMR spectra were recorded at 22°C on Bruker DRX 600 or DRX 800 NMR spectrometers. Spectra were processed with NMRPIPE (*30*) and analyzed using XEASY (*31*). Backbone and side chain ^1H, ^{15}N and ^{13}C resonances were assigned using standard triple resonance experiments (*12*). Distance restraints were derived from ^{13}C- and ^{15}N-edited 3D NOESY experiments. Assignments for the RNA were obtained from 2D isotope-filtered experiments. Intermolecular distance restraints were measured in 3D ^{13}C-edited/filtered experiments (*11, 12*). Dihedral angle restraints for the backbone angle φ were derived from $^3J(H^N,H^\alpha)$ coupling constants measured in an HNHA-J experiment (*32*); additional φ/ψ restraints were derived from TALOS (*33*). Hydrogen bond restraints for secondary structure elements in the protein were defined from slowly exchanging amide protons, identified after exchange of the H_2O buffer to D_2O. For NMR titrations, chemical shifts were recorded with ^1H,^{15}N-HSQC (heteronuclear single-quantum correlation) experiments on a 600-MHz spectrometer using 1 mM ^{15}N-labeled NMR samples of SF1 proteins comprising the KH, KH-QUA2, and KH-QUA2-Zn regions. The experimentally determined distance restraints (2855 NOEs, including 175 RNA/RNA, 298 protein/RNA, and 76 hydrogen bond restraints) and dihedral angle (169) restraints were applied in a mixed torsion angle/Cartesian dynamics simulated annealing protocol using CNS (*34*) and ARIA (*35*). The simulated annealing protocol was greatly extended compared to standard protein structure calculations. NOEs involving the RNA were manually assigned and calibrated. A floating chirality approach (*36*) was used to define stereospecific assignments of isopropyl groups. Structural quality was evaluated using PROCHECK (*37*). In the final ensemble of 10 NMR structures, the atomic root-mean-square deviation (rmsd) about the mean coordinate positions is 0.60 ± 0.17 for the backbone and 1.37 ± 0.28 for all heavy atoms excluding loop regions. No distance restraint is violated by more than 0.4 Å. Deviations from experimental distance, dihedral and residual dipolar coupling restraints are 0.0027 ± 0.0009 Å and 0.49 ± 0.08°, respectively. Deviations from idealized covalent geometry for bond lengths, bond angles, and improper dihedral angles are 0.0032 ± 0.00006 Å, 0.458 ± 0.007°, and 0.345 ± 0.001°, respectively. 75.3 ± 2.3% and 19.5 ± 2.8% of the φ/ψ angles lie in the most favored and additionally allowed regions of the Ramachandran plot, respectively. Hydrogen bonds and electrostatic interactions are identified if the corresponding geometrical constraints are observed in more than 50% of the final NMR structures. Figures showing 3D structures and molecular surfaces were prepared using MOLMOL (*38*) and GRASP (*39*), respectively.
11. G. Varani, A. Fareed, F. H.-T. Allain, *Prog. NMR Spectrosc.* **29**, 51 (1996).
12. M. Sattler, J. Schleucher, C. Griesinger, *Prog. NMR Spectrosc.* **34**, 93 (1999).
13. H. A. Lewis *et al.*, *Cell* **100**, 323 (2000).
14. G. Musco *et al.*, *Cell* **85**, 237 (1996).
15. Z. Liu, M. J. Bottomley, A. C. Messias, R. Sprangers, M. Sattler, data not shown.
16. G. Musco *et al.*, *Nature Struct. Biol.* **4**, 712 (1997).
17. H. A. Lewis *et al.*, *Structure* **7**, 191 (1999).
18. J. P. Gallivan, D. A. Dougherty, *Proc. Natl. Acad. Sci. U.S.A.* **96**, 9459 (1999).
19. N. Handa *et al.*, *Nature* **398**, 579 (1999).
20. C. Oubridge, N. Ito, P. R. Evans, C. H. Teo, K. Nagai, *Nature* **372**, 432 (1994).
21. Other KH domains also bind small (three to four nucleotides) single-stranded RNA elements, most of which contain adenosine residues (*17*). RNA binding of the STAR protein Sam68 is abolished upon mutation of the third adenosine in the tetranucleotide sequence Ura-Ade-Ade-Ade (*40*). These KH domains could thus employ similar modes of adenosine recognition.
22. Recognition of the BPS RNA by SF1 involves residues which are characteristic for STAR family proteins. For example, K184, which contacts Ade7, is a conserved residue at the beginning of a STAR protein-specific extension of the variable loop (*6*). The K184A mutation abolishes BPS binding (Fig. 4), and the corresponding R185C mutation in the STAR protein How/Who induces an embryonic lethal phenotype in *Drosophila* (*41*) demonstrating the importance of this residue. In contrast, in the Nova2-KH3/RNA complex Cyt13 (which corresponds to Ade7 in the BPS) is recognized by a residue (R54) in strand β3 (*13*). Given the conservation of the SF1 KH-QUA2 region among members of the STAR family and the importance of STAR-specific residues for RNA binding, it is likely that other STAR family proteins recognize single-stranded RNA in a similar way.
23. J. Valcárcel, R. K. Gaur, R. Singh, M. R. Green, *Science* **273**, 1706 (1996).
24. C. C. Query, M. J. Moore, P. A. Sharp, *Genes Dev.* **8**, 587 (1994).
25. J. A. Berglund, M. Rosbash, S. C. Schultz, *RNA* **7**, 682 (2001).
26. B. Rutz, B. Seraphin, *RNA* **5**, 819 (1999).
27. S. Guth, J. Valcárcel, *J. Biol. Chem.* **275**, 38059 (2000).
28. A. De Klein *et al.*, *Hum. Mol. Genet.* **7**, 393 (1998).
29. J. A. Kuivenhoven *et al.*, *J. Clin. Invest.* **98**, 358 (1996).
30. F. Delaglio *et al.*, *J. Biomol. NMR* **6**, 277 (1995).
31. C. Bartels, T.-H. Xia, M. Billeter, P. Güntert, K. Wüthrich, *J. Biomol. NMR* **5**, 1 (1995).
32. H. Kuboniwa, S. Grzesiek, F. Delaglio, A. Bax, *J. Biomol. NMR* **4**, 871 (1994).
33. G. Cornilescu, F. Delaglio, A. Bax, *J. Biomol. NMR* **13**, 289 (1999).
34. A. T. Brünger *et al.*, *Acta Crystallogr. D* **54**, 905 (1998).
35. M. Nilges, S. I. O'Donoghue, *Prog. NMR Spectrosc.* **32**, 107 (1998).
36. R. H. Folmer, C. W. Hilbers, R. N. Konings, M. Nilges, *J. Biomol. NMR* **9**, 245 (1997).
37. R. A. Laskowski, J. A. Rullmannn, M. W. MacArthur, R. Kaptein, J. M. Thornton, *J. Biomol. NMR* **8**, 477 (1996).
38. R. Koradi, M. Billeter, K. Wüthrich, *J. Mol. Graph.* **14**, 51 (1996).
39. A. Nicholls, K. A. Sharp, B. Honig, *Proteins Struct. Function Genet.* **11**, 282 (1991).
40. Q. Lin, S. J. Taylor, D. Shalloway, *J. Biol. Chem.* **272**, 27274 (1997).
41. E. H. Baehrecke, *Development* **124**, 1323 (1997).
42. Single-letter abbreviations for the amino acid residues are as follows: A, Ala; C, Cys; D, Asp; E, Glu; F, Phe; G, Gly; H, His; I, Ile; K, Lys; L, Leu; M, Met; N, Asn; P, Pro; Q, Gln; R, Arg; S, Ser; T, Thr; V, Val; W, Trp; and Y, Tyr.

43. We thank J. Valcarcel and I. Mattaj for suggestions and critical reading of the manuscript; the European Large Scale facility in Frankfurt, Germany, and W. Bermel (Bruker, Karlsruhe, Germany) for time on the 800-MHz spectrometer; and M. Nilges and J. Linge for ARIA software. Support from EMBL and the Deutsche Forschungsgemeinschaft (M.S.); Fonds voor Wetenschappelijk Onderzoek (FWO), Vlaanderen, Netherlands, and European Molecular Biology Organization (I.L.); Fundação para a Ciência e Tecnologia (A.C.M.); and the Swiss National Science Foundation (SNF) and the Canton of Geneva (A.K.) is acknowledged. Coordinates for the NMR structure of the SF1/RNA complex have been deposited in the Protein Data Bank under accession code 1K1G.

25 July 2001; accepted 13 September 2001

Mammalian TOR: A Homeostatic ATP Sensor

Patrick B. Dennis,[1] Anja Jaeschke,[1] Masao Saitoh,[1] Brian Fowler,[2] Sara C. Kozma,[1] George Thomas[1]*

The bacterial macrolide rapamycin is an efficacious anticancer agent against solid tumors. In a hypoxic environment, the increase in mass of solid tumors is dependent on the recruitment of mitogens and nutrients. When nutrient concentrations change, particularly those of essential amino acids, the mammalian Target of Rapamycin (mTOR) functions in regulatory pathways that control ribosome biogenesis and cell growth. In bacteria, ribosome biogenesis is independently regulated by amino acids and adenosine triphosphate (ATP). Here we demonstrate that the mTOR pathway is influenced by the intracellular concentration of ATP, independent of the abundance of amino acids, and that mTOR itself is an ATP sensor.

The survival of organisms is dependent on their ability to maintain cellular homeostasis. Environmental cues are deciphered by cellular regulatory elements, which adjust an organism's metabolic state to reflect external conditions. The phosphatidylinositide kinase–related family of protein kinases contains a number of critical effectors that sense environmental factors that control the ability of an organism to survive. One member of the family is mTOR, which resides at the interface between nutrient sensing and the regulation of major metabolic responses (*1–3*). Depending on mitogen and amino acid availability, mTOR positively regulates translation and ribosome biogenesis while negatively controlling autophagy (*1*), suggesting that mTOR sets protein synthetic rates as a function of the availability of translational precursors (*4*, *5*). In response to mitogens and amino acids, mTOR phosphorylates and controls the activities of two key translational regulators, S6 kinase 1 (S6K1) and initiation factor 4E binding protein (4E-BP1) (*2*). However, changes in mTOR activity in vitro, after either mitogen or amino acid treatment, have been small and controversial (*2*, *3*). The importance of understanding the molecular mechanisms that control mTOR function is underscored by recent phase 1 clinical trials showing that rapamycin is efficacious in the treatment of solid tumors in patients with metastatic renal cell carcinoma and non–small cell lung, prostate, and breast cancer (*6*).

Protein synthesis is the major energy-consuming process in the cell (*7*). In bacteria, protein synthesis and cell growth are linked by ribosome biogenesis, which is independently controlled by amino acid and adenosine triphosphate (ATP) availability (*8*). Because mTOR is sensitive to amino acids and regulates ribosome biogenesis (*1–3*), we tested its activity for sensitivity to alterations in intracellular ATP concentrations. We used insulin-induced S6K1 activation and 4E-BP1 phosphorylation as reporters for mTOR function in the presence of glycolytic or mitochondrial inhibitors (*9*). The glycolytic inhibitor 2-deoxyglucose (2-DG) was more effective in inhibiting S6K1 Thr^{389} phosphorylation and S6K1 activation than was the mitochondrial inhibitor rotenone (Fig. 1A). Similar results were obtained when an mTOR-mediated phosphorylation site in 4E-BP1 (Ser^{65}) was measured (Fig. 1B) and when iodoacetic acid and dinitrophenol were used as glycolytic and mitochondrial inhibitors, respectively (*10*). The effectiveness of each agent in inhibiting S6K1 activation par-

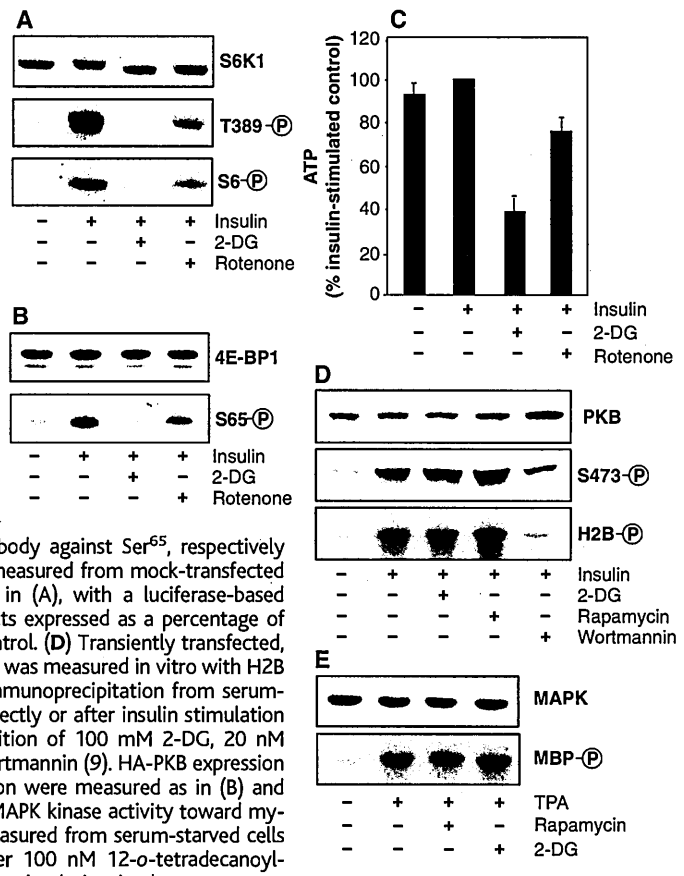

Fig. 1. The effects of metabolic inhibitors. **(A)** Serum-starved HEK293 cells were extracted directly or stimulated with 200 nM insulin in the presence of 100 mM 2-DG or 20 μM rotenone for 30 min. S6K1 levels and Thr^{389} phosphorylation were measured by Western blot analysis (*9*). S6K1 activity was assayed as described previously (*22*). **(B)** The expression and phosphorylation of transiently transfected HA-4E-BP1 was measured as in (A), with a polyclonal antibody to HA and phosphospecific antibody against Ser^{65}, respectively (*9*). **(C)** ATP levels were measured from mock-transfected HEK293 cells treated as in (A), with a luciferase-based assay (*11*), with the results expressed as a percentage of the insulin-stimulated control. **(D)** Transiently transfected, HA-tagged PKB activation was measured in vitro with H2B as substrate (*22*) after immunoprecipitation from serum-starved cells extracted directly or after insulin stimulation with or without the addition of 100 mM 2-DG, 20 nM rapamycin, or 100 nM wortmannin (*9*). HA-PKB expression and Ser^{473} phosphorylation were measured as in (B) and (*9*), respectively. **(E)** HA-MAPK kinase activity toward myelin basic protein was measured from serum-starved cells extracted directly or after 100 nM 12-*o*-tetradecanoylphorbol-13-acetate (TPA) stimulation in the presence or absence of 20 nM rapamycin or 100 mM 2-DG for 30 min (*22*). All results and the SE in (C) are representative of at least three independent experiments.

[1]The Friedrich Miescher Institute for Biomedical Research, Maulbeerstrasse 66, CH–4058, Basel, Switzerland. [2]University Childrens Hospital CH–4005, Basel, Switzerland.

*To whom correspondence should be addressed. E-mail: gthomas@fmi.ch